

Article

Enhancing Mechanical Response of Monolithic Magnesium Using Nano-NiTi (Nitinol) Particles

Gururaj Parande ¹, Vyasaraj Manakari ¹, Saif Wakeel ², Milli Suchita Kujur ^{1,3} and Manoj Gupta ^{1,*}

¹ Department of Mechanical Engineering, National University of Singapore, 9 Engineering Drive 1, Singapore 117576, Singapore; gururaj.parande@u.nus.edu (G.P.); mbvyasaraj@u.nus.edu (V.M.); millisuchitakujur@gmail.com (M.S.K.)

² Department of Mechanical Engineering, Aligarh Muslim University, Aligarh 202002, India; saifwakeel@gmail.com (S.W.)

³ Department of Mechanical Engineering, Indian Institute of Technology (ISM), Dhanbad 826004, Jharkhand, India

* Correspondence: mpegm@nus.edu.sg; Tel.: +65-651-635-8

Received: 25 October 2018; Accepted: 28 November 2018; Published: 2 December 2018



Abstract: The present study focuses on investigating the effects of Nickel-Titanium (NiTi) nanoparticles on the microstructure and properties of pure Mg. Mg composites containing varying weight percentages (0.5, 1, 1.5, 3) of NiTi nanoparticles were fabricated using Disintegrated Melt Deposition (DMD), followed by hot extrusion. The synthesized materials were characterized in order to investigate their physical, microstructural and mechanical properties. Synthesized materials were characterized for their density and porosity levels, microstructural characteristics, and mechanical response. Superior grain refinement was realized by the presence of NiTi nanoparticles in the magnesium matrix. The addition of NiTi nanoparticles resulted in strength property enhancements of pure Mg with minimal adverse effect on the ductility. Structure-property evaluations are detailed in the current study.

Keywords: magnesium; disintegrated melt deposition; compressive properties; tensile properties; metal matrix nanocomposites; NiTi

1. Introduction

Magnesium (Mg) is a non-ferrous, alkaline earth metal found in Group II of the periodic table and it is one of the lightest engineering metals (33% lighter than aluminum) with a density of approximately 1.74 g/cc [1]. It is gaining interest in engineering applications where weight saving is a critical design consideration. Lighter materials save energy, which would translate into cost savings for both the company and the end user. Mg also exhibits other desirable characteristics such as high specific strength, good thermal conductivity, high damping capacity, and castability. However, due to low ductility, limited absolute strength, modulus of elasticity and corrosion resistance, Mg cannot be extensively used in many structural applications in its pure form [2]. The most commonly used methods to address these limitations are: (a) alloying; (b) composite technology; and (c) surface protection by means of coating. Alloying is commonly used to improve the room temperature properties of Mg and commonly used alloying materials are aluminum, zinc, manganese, zirconium, and rare earth elements [3–6]. However, there are some drawbacks associated with alloying as the alloying elements can lead to an appreciable increase in the density of the material. Further, some alloying elements (such as Al) are neurotoxic which restricts the widespread applications of these alloys, especially in the biomedical sector. Addition of inexpensive secondary reinforcements into the

Mg matrix greatly enhances the mechanical properties such as strength and stiffness. Thus, magnesium matrix composites (MMCs) are widely being used due to their better mechanical properties as compared to pure metals [1,7–10]. In addition, many novel and advanced materials have been developed based on the various types of matrix and reinforcements. Limited content (<3%) of nano-length scale reinforcements into magnesium has been shown to improve the mechanical properties without significantly altering the density of the developed material [11]. Critically optimized techniques are required to add the nano-scale reinforcements to the Mg matrix for making Mg-base nano-composites. The Disintegrated Melt Deposition (DMD) technique was first developed by Gupta et al. [12], which is a modification of spray atomization and deposition technique. The DMD method brings together the cost-effectiveness of conventional casting and the scientific innovativeness and technological potential of the spray process. Moreover, unlike the spray process, the DMD technique uses lower impinging gas jet velocity which results in a high yield with a uniform distribution of reinforcement. The composite material ideally should exhibit a uniform distribution of ceramic reinforcement and good metal-reinforcement interfacial bonding. The DMD technique has been successfully used to synthesize a wide range of magnesium-based composites [13–16]. This method is also capable of producing composites of finer grain size. Further, material wastage associated with the DMD method is also 20 to 30% less than those associated with conventional casting [17]. Recent studies on DMD fabricated Mg nanocomposites with different reinforcements (SiC, B₄C, SiO₂, TiO₂, Al₂O₃ and so on) have reported superior enhancement in the mechanical and ignition properties of magnesium in the presence of nanoparticles [1,9,18–23]. However, no attempt has been yet made to investigate NiTi as a reinforcement for fabricating Mg metal matrix nanocomposites. Superelasticity and one-way shape-memory effect displayed by the NiTi [24–29] makes it an often-used metallic material for shape memory applications. Nitinol, as it is commonly referred to commercially, has a moderate solubility range, when alloyed with light metals like Mg, Al can effectively enhance the shape memory and mechanical properties. Key properties like high fatigue strength, excellent corrosion resistance, high damping capacities below transition temperatures and moderate-to-high impact resistance makes it a viable option to explore for materials targeting aerospace and biomedical sectors [25,26,30,31]. Superior functional capability and biocompatibility coupled with lower elastic modulus matching the bone make NiTi an attractive option for surgical tools, orthodontic wires and cardiovascular stents [32,33].

The present study was conducted with the prime objective to investigate the mechanical properties of magnesium composites containing NiTi nanoparticles in different amounts (0.5, 1, 1.5, 3 wt. %). The composites were synthesized using the DMD method followed by hot extrusion. Subsequently, physical, mechanical, and microstructural characterization tests were conducted, which include density and porosity measurements, optical and scanning electron microscopy examinations, tensile tests, compression tests and fracture studies of tensile and compressive failed samples.

2. Materials and Methods

2.1. Materials and Processing

Mg turnings with 99.9% purity supplied by ARCOS Organics, Morris Plains, NJ, USA were used as a base metal and 99.9% pure Ni-Ti powder of size 30–120 nm from US Research Nanomaterials, Houston, TX, USA was used as a reinforcement.

Five castings were made using the DMD technique. Pure Mg and (0.5, 1, 1.5 and 3 wt. %) NiTi were placed in a multilayered arrangement in a graphite crucible and superheated to 750 °C in the presence of argon gas using a resistance heating furnace. For uniform distribution of reinforcement within the magnesium matrix, the superheated slurry was stirred at 450 rpm for 5 min. After adequate stirring, molten metal was then allowed to pour down into the steel mold. Before entering into the mold, molten metal was disintegrated by two jets of argon gas (flow rate of 25 lpm) and finally, an ingot of 40 mm diameter was obtained. An experimental setup of DMD is shown in Figure 1.

The hot extrusion parameters selected in the present work were based on past research. Extrusion was carried at 350 °C at an extrusion ratio of 20.25:1 yielding 8 mm rod. During hot extrusion, there was no severe increase in pressure, which validates that appropriate parameters were selected.

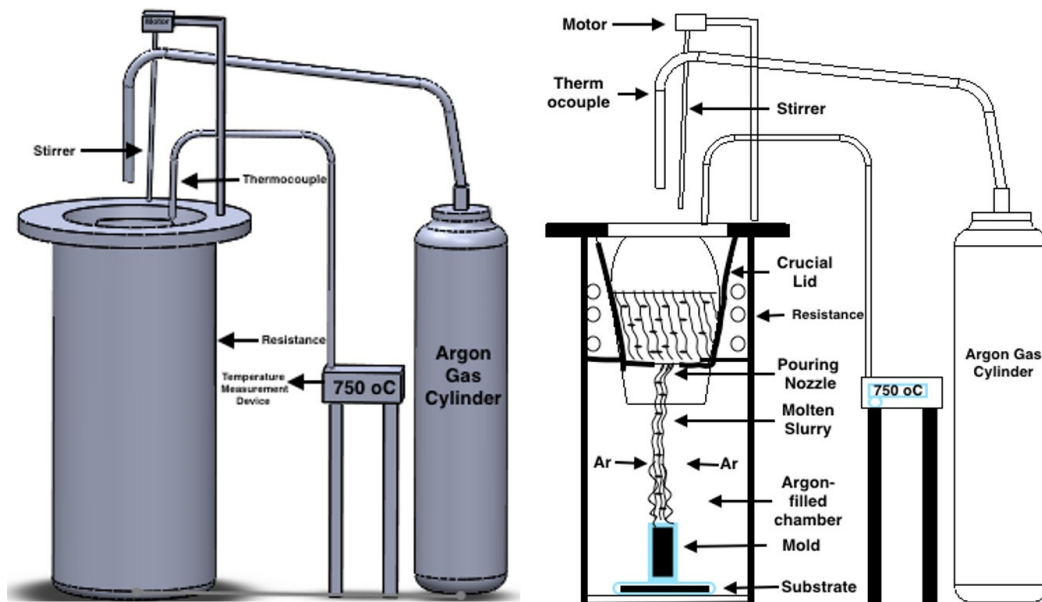


Figure 1. Experimental setup of the DMD method.

2.2. Material Characterization

2.2.1. Density Measurements

The density of pure Mg and Mg-nanocomposite reinforced with a different composition of NiTi was calculated by using the Archimedes principle. Four polished samples (using alumina suspension as polishing agent) were randomly selected from 8mm extruded rods of pure Mg and Mg-NiTi nanocomposite. Distilled water was used as the immersion fluid. Samples were weighed in both air and water using an A&D GR-200 electronic balance with an accuracy of ± 0.0001 g.

2.2.2. Microstructural Characterization

Microstructural characterization was performed to calculate the average grain size and the distribution of NiTi nanoparticles in the magnesium matrix was examined as per ASTM standard ASTM E112–13. Samples with different amounts of NiTi were polished with alumina suspension (5, 1, 0.3, 0.05 μm) and examined under the digital optical microscope with Scion image 4.0.3.2 analysis software (Scion Corporation, Sacramento, CA, USA) to investigate the grain distribution. JEOL JSM-5800 LV Scanning Electron Microscope (SEM, Kyoto, Japan) was used for investigating the distribution of NiTi particles.

Pure Mg and Mg-NiTi nanocomposite (0.5, 1, 1.5 and 3 wt. %) were exposed to Cu K_{α} radiation wavelength of 1.5418 Å with a scan speed of 2°/min by using an automated Shimadzu Lab-X XRD-6000 Diffractometer (Kyoto, Japan). Further, the basal plane orientation of Mg nanocomposite was analyzed with the help of an X-ray diffraction peak both in parallel and perpendicular to the extrusion axis and compared with the JCPDS data to identify the possible secondary phases formed.

2.2.3. Coefficient of Thermal Expansion

The coefficient of thermal expansion (CTE) of the extruded monolithic and Mg-NiTi nanocomposites was determined using LINSEIS TMA PT 1000LT thermomechanical analyzer

(Tokyo, Japan) with a gas flow rate of 0.1 lpm at a rate of heating of 5 °C/min and the displacements of the samples with respect to the temperature (50–350 °C) were recorded.

2.2.4. Mechanical Properties

Microhardness of the samples was measured as per ASTM E384-08 using a Shimadzu HMV automatic digital hardness tester (Tokyo, Japan) at 25 gf load and 15 s dwell time. Five samples were tested per composition and the measurements were done in a concentrated area to ensure conformance.

To investigate the compressive properties, quasi-static compression tests were conducted as per ASTM E9-89a. At room temperature, cylindrical samples with $\Phi 8 \text{ mm} \times 8 \text{ mm}$ were tested using 810 MTS (Material testing System) under the strain rate of $8.3 \times 10^{-5} \text{ s}^{-1}$. A minimum of five samples were tested to ensure consistent and reproducible results.

The tensile properties were determined in accordance with the ASTM test standard E8M-08 at ambient temperature by employing the 810 Material Test System (MTS). Samples were prepared with 25 mm gauge length and 5 mm diameter. The strain rate was set at 0.01 min^{-1} and an Instron 2630-100 series extensometer (Singapore) to measure the failure strain. A minimum of five tensile tests was conducted for each material in order to ensure the consistency of results.

JEOL JSM-5800 LV Scanning Electron Microscope (SEM, Kyoto, Japan) was used to analyze fractured samples for investigating the mode of failure under compression and tensile loading.

3. Results and Discussion

3.1. Density and Porosity

The results of density and porosity are shown in Table 1. With the addition of NiTi in Mg matrix, an increase in the experimental density is observed when compared to that of Pure Mg. Theoretical density is calculated as per the rule of mixtures. Mg₃NiTi displayed the highest theoretical density of 1.78 g/cc, which is ~2.4% increase in density as compared to that of pure Mg. The increase in experimental and theoretical density can be attributed to the density difference between pure Mg (1.74 g/cc) and NiTi (6.45 g/cc). Further, reduced porosity in the case of nanocomposites when compared to pure Mg may be attributed to good wettability between NiTi nanoparticles and pure Mg in liquid and solid states. There was no visible evidence of any macrostructural defects after extrusion. Extruded rods were shiny and smooth without any visible circumferential cracks. In addition, low porosity values (<1%) displayed by monolithic and nanocomposite samples indicates that the DMD process coupled with hot extrusion is a suitable methodology for the synthesis of Mg-based composites.

Table 1. Density and porosity of pure Mg and Mg-NiTi nanocomposites.

Material	Theoretical Density (g/cc)	Experimental Density (g/cc)	Porosity (%)
Pure Mg	1.73	1.72 ± 0.025	0.85
Mg _{0.5} NiTi	1.74	1.73 ± 0.008	0.48
Mg ₁ NiTi	1.75	1.74 ± 0.002	0.51
Mg _{1.5} NiTi	1.75	1.75 ± 0.003	0.50
Mg ₃ NiTi	1.78	1.76 ± 0.008	0.67

3.2. Microstructural Characterisation

The grain size of pure Mg and Mg nanocomposites is presented in Table 2 and the representative grain morphologies are presented in Figure 2a–c. The grain size of pure Mg was significantly refined with the presence of NiTi nanoparticles. Mg_{0.5}NiTi, Mg₁NiTi, Mg_{1.5}NiTi and Mg₃NiTi nanocomposite showed a grain size of 17, 13, 10 and 9 μm , respectively compared to pure Mg (40 μm). Presence of ~0.5 wt. % NiTi was effective to refine the grain size of Mg by ~60%. The grain refinement with the progressive addition of nanoparticles is also significant as the average grain size of Mg₃NiTi

is approximately half the size of Mg0.5NiTi nanocomposite. Refining of grain size is crucial as the strength and corrosion properties of Mg-based materials greatly depends on the grain size of the material. The decrease in grain size can be mainly attributed to the ability of fine NiTi nanoparticles to pin the grain boundaries in the Mg matrix [34,35].

Table 2. Grain size, CTE and microhardness of Mg-NiTi nanocomposite samples.

Material	Grain Size (μm)	CTE ($\times 10^{-6}/\text{K}$)	Microhardness (Hv)
Pure Mg	40 ± 9.4	27.1	57 ± 4.6
Mg0.5NiTi	17 ± 2.2 (60%↓)	26.4 (3%↓)	59 ± 3.3 (4%↑)
Mg1NiTi	13 ± 1 (67%↓)	25.9 (4%↓)	72 ± 2.5 (26%↑)
Mg1.5NiTi	10 ± 3.3 (75%↓)	25.6 (5%↓)	73 ± 3.9 (28%↑)
Mg3NiTi	9 ± 1.8 (76%↓)	24.3 (10%↓)	75 ± 2.6 (31%↑)

Figure 2d shows a representative image of reasonably uniform distribution and minimum clustering of the reinforcement particles in the Mg1.5NiTi nanocomposite. The phases formed cannot be particularly identified in the SEM but can be confirmed by the X-ray diffraction (XRD) analysis. The reasonably uniform distribution of the NiTi nanoparticles and secondary phases can be attributed to (a) optimal processing parameters (b) effect of Ar disintegration on the melt stream and (c) high extrusion ratio to breakdown hard phases and clusters.

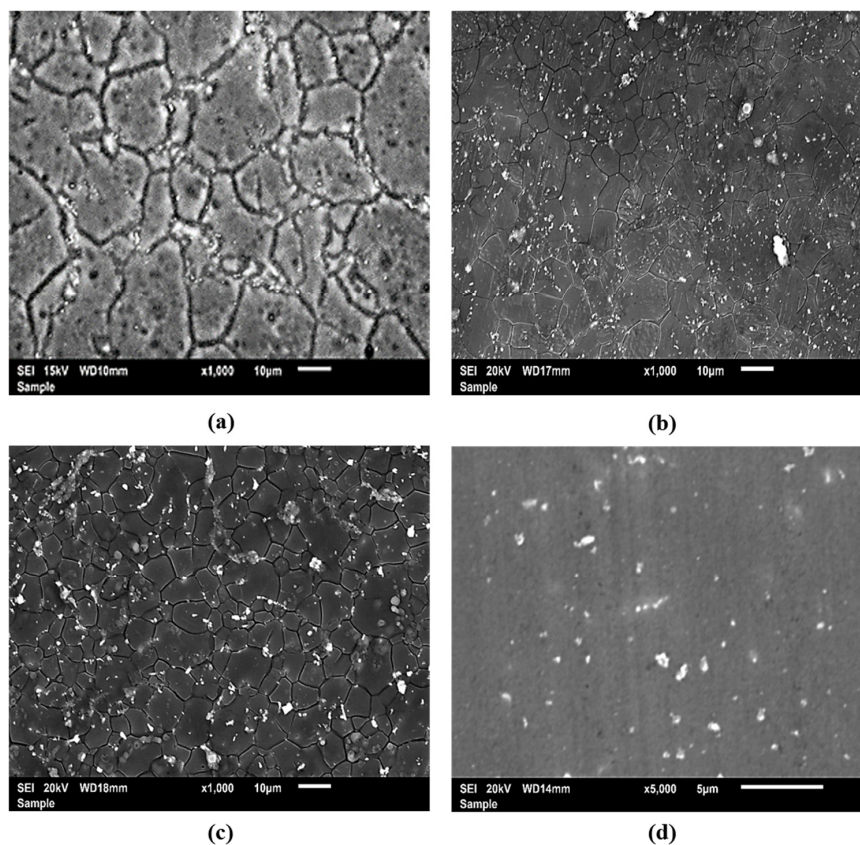


Figure 2. Grain size of (a) pure Mg, (b) Mg1.5NiTi, (c) Mg3NiTi; (d) NiTi distribution in the Mg matrix.

X-ray diffractograms of Pure Mg and Mg-NiTi nanocomposites obtained from the longitudinal sections of the extruded samples are shown in Figure 3. The high-intensity peaks of Mg are clearly visible in the diffractograms. Also, there are peaks other than Mg that correspond to the presence of other phases in the sample. Few peaks of NiTi reinforcement is observed in the XRD analysis. Pure Mg is known to have a predominantly basal texture. Due to this basal texture, the deformation behavior of magnesium-based materials is very complicated to understand. However, clear peaks of NiTi are not observed due to the limitation of the filtered X-ray [11] to detect smaller weight fraction nanoparticle additions. Pure Mg, Mg0.5Ti, Mg1.5NiTi and Mg3NiTi exhibited a strong basal texture as the intensity corresponding to the basal plane (Theta-2Theta = 34 deg.) is maximum in the aforementioned compositions. Randomized texture was only observed in the case of Mg1NiTi composite owing to the maximum intensity corresponding to the pyramidal plane (Theta-2Theta = 36 deg.). Randomization in texture of Mg1NiTi nanocomposite leads to the basal plane remaining tilted and not parallel to the extrusion axis. This phenomenon improves the plastic deformation of the material which is representative of Mg1NiTi nanocomposite having higher fracture strain values than other nanocomposites under compression mode. Formation of other phases which includes Mg₂Ni and Ti₂Ni (Figure 3) at various angles was also observed [27,36].

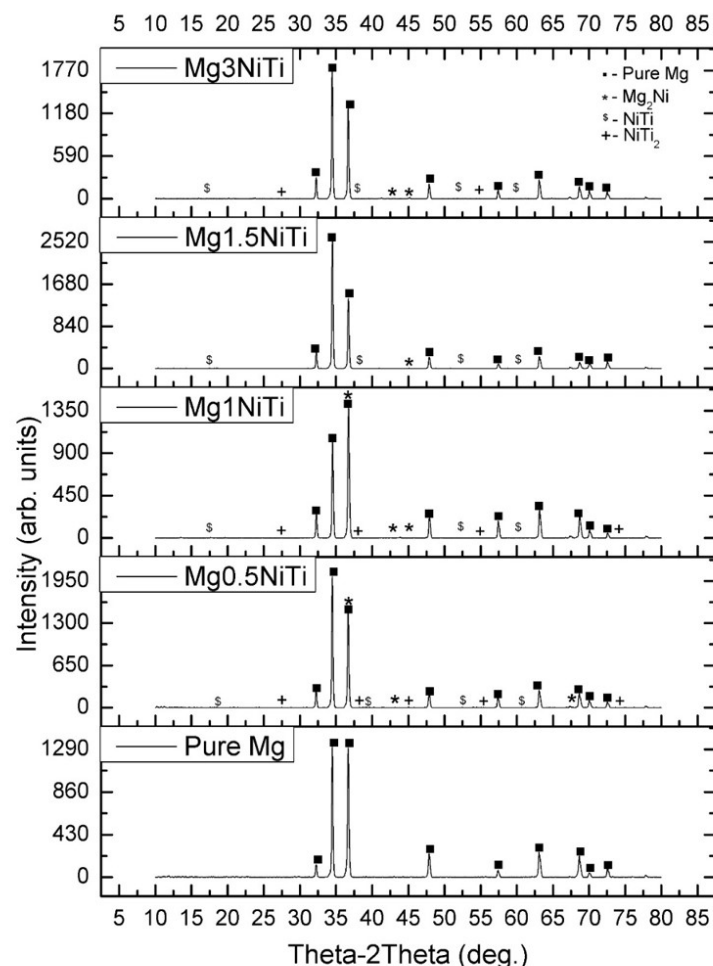


Figure 3. Longitudinal section of pure Mg and Mg-NiTi nanocomposites.

3.3. Coefficient of Thermal Expansion

The results of the coefficient of thermal expansion (CTE), represented in Table 2, show that with progressive addition of NiTi in pure Mg matrix, CTE decreases. The CTE of pure Mg was observed to be $27.1 \times 10^{-6}/\text{K}$. Mg0.5NiTi, Mg1NiTi, Mg1.5NiTi and Mg3NiTi nanocomposites exhibited the

CTE value of $26.4 \times 10^{-6}/\text{K}$, $25.9 \times 10^{-6}/\text{K}$, $25.6 \times 10^{-6}/\text{K}$, and $24.3 \times 10^{-6}/\text{K}$, respectively. The experimental CTE values were in close agreement with the theoretical CTE values as calculated by the Turner model [37]. The relatively lower CTE values might be attributed to the lower CTE of the NiTi reinforcement ($\sim 10 \times 10^{-6}/\text{K}$) [38].

3.4. Mechanical Properties

Microhardness values of the samples are presented in Table 2. Addition of NiTi in the Mg matrix enhanced the microhardness value and maximum microhardness was observed in Mg₃NiTi (75 Hv), which is $\sim 31\%$ greater than that of pure Mg (57 Hv). The increase in hardness of Mg-NiTi nanocomposites can be attributed to their lower grain size (Table 2) and higher hardness of NiTi particles (~ 600 Hv), which lead to more resistance to the localized deformation of the matrix during indentation [39].

Tensile properties of the Mg-NiTi nanocomposites are shown in Table 3. The addition of NiTi improves the tensile yield strength (0.2% TYS) and ultimate tensile strength (UTS) of the Mg nanocomposite. Further, Mg₃NiTi exhibited the maximum 0.2% TYS and UTS of 193 MPa and 217 MPa, which is $\sim 129\%$ and $\sim 46\%$ greater than that of pure Mg (84 MPa & 148 MPa), respectively. Tensile stress-strain response of pure Mg and Mg-NiTi nanocomposites are shown in Figure 4a.

Table 3. Room temperature tensile testing results.

Material	0.2% TYS (MPa)	UTS (MPa)	Fracture Strain (%)	Energy Absorbed (MJ/m ³)
Pure Mg	84 ± 6	148 ± 6	13 ± 0.9	17 ± 1.5
Mg _{0.5} NiTi	106 ± 12 (26%↑)	167 ± 14 (13%↑)	9 ± 0.8	24 ± 1.8 (41%↑)
Mg ₁ NiTi	123 ± 2 (47%↑)	176 ± 9 (19%↑)	9 ± 4.2	14 ± 1.6
Mg _{1.5} NiTi	163 ± 9 (94%↑)	187 ± 8 (26%↑)	9 ± 0.4	14 ± 2.1
Mg ₃ NiTi	193 ± 17 (129%↑)	217 ± 16 (46%↑)	11 ± 0.2	23 ± 2.4 (35%↑)

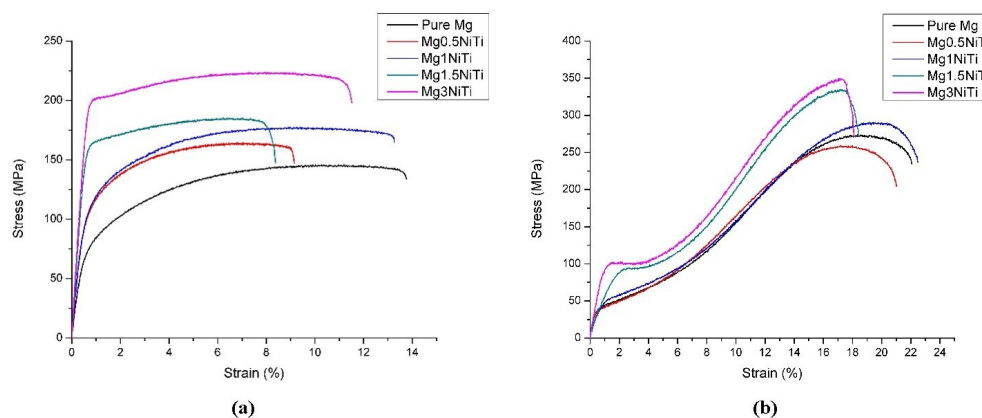


Figure 4. (a) Tensile and (b) compressive stress vs. strain curve obtained for different Mg-NiTi nanocomposites.

The superior and progressive enhancement in the strength properties of the nanocomposites may be attributed to: (a) the decreasing grain size of the Mg-NiTi nanocomposites, (b) Orowan strengthening mechanism [40,41], and (c) increase in dislocation density in the matrix during primary/secondary processing due to variation in CTE of matrix and reinforcement [42]. The load transfer capabilities

and strengthening owing to the difference in elastic modulus are found to be limited mainly in lower weight fraction additions as compared to Hall–Petch, Orowan and Forest strengthening [43,44].

Tensile testing results also revealed that ductility of Mg–NiTi composites remained in 9–11% marginally lower than 13% exhibited by pure Mg. The energy absorbed until fracture under tensile mode enhanced with the addition of 0.5 wt. % NiTi nanocomposite. A slight decrease was observed with the addition of 1 and 1.5 wt. % NiTi nanoparticles owing to their reduced fracture strain values. Further addition of 3 wt. % NiTi addition exhibited an increased energy absorption value of 23 MJ/m³ which is ~35% greater than pure Mg (17 MJ/m³). This can be primarily attributed to the inability of NiTi to randomize the texture in most cases and the increasing presence of harder phases (NiTi, Mg₂Ni and NiTi₂) in the matrix (see Figures 2 and 3) leading to a relatively early crack nucleation and faster crack growth due to higher hardness of the matrix (Table 2). Tensile fractography results are shown in Figure 5. The fracture surface of pure Mg (Figure 5a), Mg0.5NiTi (Figure 5b), and Mg1NiTi (Figure 5c) samples indicates a cleavage mode of fracture highlighting that the fracture behavior of the synthesized nanocomposites is greatly controlled by the Mg matrix material. The cleavage steps as seen in these tensile fractographs are the indications of the inability of uniform deformation Mg based materials due to basal slip [45,46]. However, increasing amount of NiTi nanoparticles progressively refined the fracture features and a mixed mode of fracture with both cleavage and signs of plastic deformation were observed along with the cracks in the magnesium metal matrix for Mg1.5NiTi (Figure 5d) and Mg3NiTi (Figure 5e) nanocomposites.

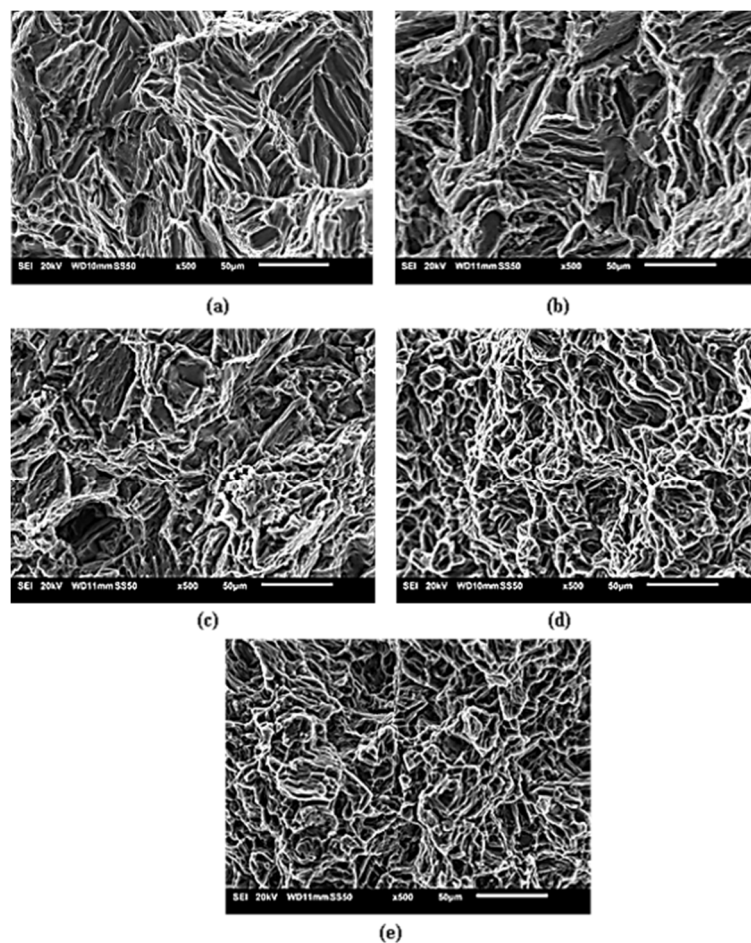


Figure 5. Tensile fractography of (a) Pure Mg, (b) Mg0.5NiTi, (c) Mg1NiTi, (d) Mg1.5NiTi and (e) Mg3NiTi nanocomposites.

Compressive test results are shown in Table 4 and representative curves are shown in Figure 4b. It can be observed that the presence of NiTi nanoparticles resulted in superior strength properties in compression mode. Increased 0.2% compressive yield strength (0.2% CYS) and ultimate compressive strength (UCS) properties are observed. 0.2% CYS of pure Mg (46 MPa) was improved by the addition of 1, 1.5, and 3 wt. % NiTi resulting in strength values of 52, 78, and 94 MPa, respectively. Similarly, UCS of Mg1NiTi (290 MPa), Mg1.5NiTi (337 MPa) and Mg3NiTi (345 MPa) nanocomposites are a 6%, 23%, and 24% enhancement, respectively compared to base pure Mg (274 MPa). A slight anomaly is observed for Mg0.5NiTi nanocomposites with respect to the strength properties. This can be attributed to the fact that the amount is very small and acted as an impurity resulting in stress concentration sites resulting in slightly lower properties under compression mode [47].

Table 4. Room temperature compressive testing results.

Material	0.2% CYS (MPa)	UCS (MPa)	Fracture Strain (%)	Energy Absorbed (MJ/m ³)
Pure Mg	46 ± 2	274 ± 4	23 ± 0.9	39 ± 2.7
Mg0.5NiTi	42 ± 4 (9%↓)	265 ± 15 (3%↓)	23 ± 0.3	36 ± 2.4
Mg1NiTi	52 ± 6 (13%↑)	290 ± 4 (6%↑)	23 ± 0.7	40 ± 1.5
Mg1.5NiTi	78 ± 5 (70%↑)	337 ± 4 (23%↑)	18 ± 0.4	35 ± 2.1
Mg3NiTi	94 ± 3 (104%↑)	345 ± 5 (26%↑)	18 ± 0.9	35 ± 2.1

The fracture strain values of the nanocomposites were similar to the base pure Mg matrix for the NiTi content up to 1%. Beyond that ductility reduced from 23% to 18%, which is still significant from a deformation perspective and the decline can be attributed to a progressive increase in the presence of harder secondary phases (Ni₂Ti, Ni₃Ti) due to increased amounts of NiTi nanoparticles in the matrix [45]. The energy absorbed until fracture under the compression mode for pure Mg was observed to be 39 MJ/m³. EA for the developed nanocomposites were similar to the pure Mg matrix. This is due to the fact that the lower concentrations of Mg-NiTi nanocomposites have higher strength and similar ductility values when compared to pure Mg. However, enhanced additions of NiTi have higher strength but lower ductility values when compared to pure Mg. Hence, EA under compression mode does not seem any superior increment or decrement for the nanocomposites and are in each other's deviation ranges.

Fractured specimens of pure Mg and Mg-NiTi nanocomposites are shown in Figure 6. Typical shear band formations are observed, which are commonly found in other studies on Mg-based nanocomposites. All the developed nanocomposites fractured at 45° w.r.t to the test plane.

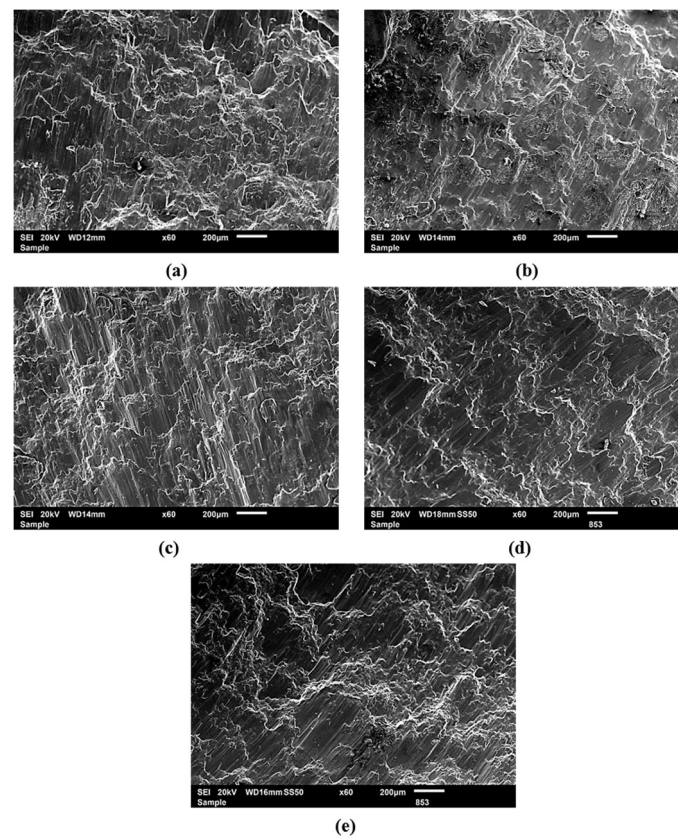


Figure 6. Compression fractography of (a) Pure Mg, (b) Mg0.5NiTi, (c) Mg1NiTi, (d) Mg1.5NiTi and (e) Mg3NiTi nanocomposites.

4. Conclusions

The current work studied the fabrication by disintegrated melt deposition (DMD) and effect of NiTi nanoparticles on magnesium nanocomposite. Mechanical, physical, and thermal properties of Mg nanocomposites have been significantly influenced by the addition NiTi. Based on the work done the following conclusions have been made:

- A. By the progressive addition of NiTi, highly dense material is obtained with limited porosity (<1%).
- B. The strong basal texture is retained in most of the Mg-NiTi nanocomposites with a high intensity corresponding to the pyramidal plane. High strength secondary phases like Mg₂Ni and NiTi₂ were formed.
- C. A near uniform distribution of NiTi nanoparticles in the magnesium matrix was observed. The NiTi nanoparticles were observed to pin the grain boundaries to restrict the grain growth and aids in the dispersion strengthening of the nanocomposite.
- D. Mg₃NiTi nanocomposite displays a near 31% enhancement in microhardness values when compared to that of pure Mg, indicating a superior response to localized plastic deformation.
- E. Improved tensile strength (both yield and ultimate) properties and improved compressive strength (both yield and ultimate) were observed with Mg₃NiTi nanocomposite displaying the maximum strength values in comparison with other developed nanocomposites.
- F. The fracture strain values for the nanocomposites in both tensile and compression mode were similar to that of pure Mg and significant enhancement or decrement was not observed.

Author Contributions: Conceptualization, M.G.; Investigation, G.P., V.M., S.W. and M.S.K.; Supervision, M.G.; Writing—original draft, G.P., V.M., S.W., M.S.K. and M.G.; Writing—review & editing, G.P., V.M. and M.G.

Conflicts of Interest: The authors declare no conflict of interest.

References

1. Guo, Y.C.; Nie, K.B.; Kang, X.K.; Deng, K.K.; Han, J.G.; Zhu, Z.H. Achieving high-strength magnesium matrix nanocomposite through synergistical effect of external hybrid (sic+tic) nanoparticles and dynamic precipitated phase. *J. Alloys Compd.* **2019**, *771*, 847–856. [[CrossRef](#)]
2. Manakari, V.; Parande, G.; Gupta, M. Selective laser melting of magnesium and magnesium alloy powders: A review. *Metals* **2016**, *7*, 2. [[CrossRef](#)]
3. Tekumalla, S.; Seetharaman, S.; Almajid, A.; Gupta, M. Mechanical properties of magnesium-rare earth alloy systems: A review. *Metals* **2014**, *5*, 1–39. [[CrossRef](#)]
4. Bohlen, J.; Yi, S.; Letzig, D.; Kainer, K.U. Effect of rare earth elements on the microstructure and texture development in magnesium–manganese alloys during extrusion. *Mater. Sci. Eng. A* **2010**, *527*, 7092–7098. [[CrossRef](#)]
5. Atrens, A.; Song, G.-L.; Liu, M.; Shi, Z.; Cao, F.; Dargusch, M.S. Review of recent developments in the field of magnesium corrosion. *Adv. Eng. Mater.* **2015**, *17*, 400–453. [[CrossRef](#)]
6. Liu, M.; Shih, D.S.; Parish, C.; Atrens, A. The ignition temperature of mg alloys WE43, AZ31 and AZ91. *Corros. Sci.* **2012**, *54*, 139–142. [[CrossRef](#)]
7. Parande, G.; Manakari, V.; Koppaarthi, S.D.S.; Gupta, M. Utilizing low-cost eggshell particles to enhance the mechanical response of Mg-2.5Zn magnesium alloy matrix. *Adv. Eng. Mater.* **2017**, *20*, 1700919. [[CrossRef](#)]
8. Huang, S.-J.; Lin, C.-C.; Huang, J.-Y.; Tenne, R. Mechanical behavior enhancement of AZ31/WS2 and AZ61/WS2 magnesium metal matrix nanocomposites. *Adv. Mech. Eng.* **2018**, *10*. [[CrossRef](#)]
9. Guo, E.; Shuai, S.; Kazantsev, D.; Karagadde, S.; Phillion, A.B.; Jing, T.; Li, W.; Lee, P.D. The influence of nanoparticles on dendritic grain growth in mg alloys. *Acta Mater.* **2018**, *152*, 127–137. [[CrossRef](#)]
10. Du, X.; Du, W.; Wang, Z.; Liu, K.; Li, S. Ultra-high strengthening efficiency of graphene nanoplatelets reinforced magnesium matrix composites. *Mater. Sci. Eng. A* **2018**, *711*, 633–642. [[CrossRef](#)]
11. Goh, C.; Wei, J.; Lee, L.; Gupta, M.J.N. Development of novel carbon nanotube reinforced magnesium nanocomposites using the powder metallurgy technique. *Nanotechnology* **2005**, *17*, 7. [[CrossRef](#)]
12. Kumar Meenashisundaram, G.; Hou Damien Ong, T.; Parande, G.; Manakari, V.; Xiang, S.; Gupta, M. Using lanthanum to enhance the overall ignition, hardness, tensile and compressive strengths of Mg-0.5Zr alloy. *J. Rare Earths* **2017**, *35*, 723–732. [[CrossRef](#)]
13. Manakari, V.; Parande, G.; Doddamani, M.; Gupta, M. Enhancing the ignition, hardness and compressive response of magnesium by reinforcing with hollow glass microballoons. *Materials* **2017**, *10*, 997. [[CrossRef](#)] [[PubMed](#)]
14. Tun, K.; Zhang, Y.; Parande, G.; Manakari, V.; Gupta, M. Enhancing the hardness and compressive response of magnesium using complex composition alloy reinforcement. *Metals* **2018**, *8*, 276. [[CrossRef](#)]
15. Parande, G.; Manakari, V.; Gupta, H.; Gupta, M. Magnesium- β -tricalcium phosphate composites as a potential orthopedic implant: A mechanical/damping/immersion perspective. *Metals* **2018**, *8*, 343. [[CrossRef](#)]
16. Jayalakshmi, S.; Sahu, S.; Sankaranarayanan, S.; Gupta, S.; Gupta, M. Development of novel Mg–Ni60Nb40 amorphous particle reinforced composites with enhanced hardness and compressive response. *Mater. Design* **2014**, *53*, 849–855. [[CrossRef](#)]
17. Gupta, M.; Parande, G.; Manakari, V. An insight into high performance magnesium alloy/nano-metastable-syntactic composites. In Proceedings of the 17th Australian International Aerospace Congress, Melbourne, Australia, 26–28 February 2017; p. 270.
18. Parande, G.; Manakari, V.; Meenashisundaram, G.K.; Gupta, M. Enhancing the tensile and ignition response of monolithic magnesium by reinforcing with silica nanoparticulates. *J. Mater. Res.* **2017**, *32*, 2169–2178. [[CrossRef](#)]
19. Meenashisundaram, G.K.; Gupta, M. Emerging environment friendly, magnesium-based composite technology for present and future generations. *JOM* **2016**, *68*, 1890–1901. [[CrossRef](#)]

20. Gupta, M.; Wong, W.L.E. Magnesium-based nanocomposites: Lightweight materials of the future. *Mater. Charact.* **2015**, *105*, 30–46. [[CrossRef](#)]
21. Kaviti, R.V.P.; Jeyasimman, D.; Parande, G.; Gupta, M.; Narayanasamy, R. Investigation on dry sliding wear behavior of Mg/Bn nanocomposites. *J. Mag. Alloys.* **2018**, *6*, 263–276. [[CrossRef](#)]
22. Kujur, M.S.; Mallick, A.; Manakari, V.; Parande, G.; Tun, K.S.; Gupta, M. Significantly enhancing the ignition/compression/damping response of monolithic magnesium by addition of Sm₂O₃ nanoparticles. *Metals* **2017**, *7*, 357. [[CrossRef](#)]
23. Kujur, M.S.; Manakari, V.; Parande, G.; Tun, K.S.; Mallick, A.; Gupta, M. Enhancement of thermal, mechanical, ignition and damping response of magnesium using nano-ceria particles. *Ceram. Int.* **2018**, *44*, 15035–15043. [[CrossRef](#)]
24. Chakif, M.; Essaidi, A.; Gurevich, E.; Ostendorf, A.; Prymak, O.; Epple, M. Generation of niti nanoparticles by femtosecond laser ablation in liquid. *J. Mater. Eng. Perform.* **2014**, *23*, 2482–2486. [[CrossRef](#)]
25. Huang, W. On the selection of shape memory alloys for actuators. *Mater. Des.* **2002**, *23*, 11–19. [[CrossRef](#)]
26. Guo, W.; Kato, H. Development of a high-damping NiTi shape-memory-alloy-based composite. *Mater. Lett.* **2015**, *158*, 1–4. [[CrossRef](#)]
27. Školáková, A.; Novák, P.; Salvetr, P.; Moravec, H.; Šefl, V.; Deduytsche, D.; Detavernier, C. Investigation of the effect of magnesium on the microstructure and mechanical properties of niti shape memory alloy prepared by self-propagating high-temperature synthesis. *Metall. Mater. Trans. A* **2017**, *48*, 3559–3569. [[CrossRef](#)]
28. Karamooz-Ravari, M.R.; Taheri Andani, M.; Kadkhodaei, M.; Saedi, S.; Karaca, H.; Elahinia, M. Modeling the cyclic shape memory and superelasticity of selective laser melting fabricated NiTi. *Int. J. Mech. Sci.* **2018**, *138–139*, 54–61. [[CrossRef](#)]
29. Taylor, S.L.; Ibeh, A.J.; Jakus, A.E.; Shah, R.N.; Dunand, D.C. NiTi-Nb micro-trusses fabricated via extrusion-based 3D-printing of powders and transient-liquid-phase sintering. *Acta Biomater.* **2018**, *76*, 359–370. [[CrossRef](#)]
30. Hao, S.; Cui, L.; Jiang, J.; Guo, F.; Xiao, X.; Jiang, D.; Yu, C.; Chen, Z.; Zhou, H.; Wang, Y. A novel multifunctional NiTi/Ag hierarchical composite. *Sci. Rep.* **2014**, *4*, 5267. [[CrossRef](#)]
31. Yuan, B.; Zhu, M.; Chung, C.Y. Biomedical porous shape memory alloys for hard-tissue replacement materials. *Materials* **2018**, *11*, 1716. [[CrossRef](#)]
32. Andani, M.T.; Moghaddam, N.S.; Haberland, C.; Dean, D.; Miller, M.J.; Elahinia, M. Metals for bone implants. Part 1. Powder metallurgy and implant rendering. *Acta Biomater.* **2014**, *10*, 4058–4070. [[CrossRef](#)] [[PubMed](#)]
33. Elahinia, M.H.; Hashemi, M.; Tabesh, M.; Bhaduri, S.B. Manufacturing and processing of NiTi implants: A review. *Progr. Mater. Sci.* **2012**, *57*, 911–946. [[CrossRef](#)]
34. Reed-Hill, R.E.; Abbaschian, R.; Abbaschian, R. *Physical Metallurgy Principles*; Cengage Learning: Stamford, CT, USA, 1973.
35. Robson, J.D.; Henry, D.T.; Davis, B. Particle effects on recrystallization in magnesium–manganese alloys: Particle-stimulated nucleation. *Acta Mater.* **2009**, *57*, 2739–2747. [[CrossRef](#)]
36. Salvetr, P.; Školáková, A.; Novak, P. Effect of magnesium addition on the structural homogeneity of NiTi alloy produced by self-propagating high-temperature synthesis. *Kovove Mater.-Metall. Mater.* **2017**, *55*, 379–383. [[CrossRef](#)]
37. Turner, P.S. *The Problem of Thermal-Expansion Stresses in Reinforced Plastics*; NACA: Washington, DC, USA, 1942.
38. Stanford, M.K. *Thermophysical Properties of 60-Nitinol for Mechanical Component Applications*; NASA: Cleveland, OH, USA, 2012.
39. Stanford, M.K. *Hardness and Microstructure of Binary and Ternary Nitinol Compounds*; NASA: Cleveland, OH, USA, 2016.
40. Aboudzadeh, N.; Dehghanian, C.; Shokrgozar, M. Synthesis, microstructure and mechanical properties of Mg₂Zn_{0.3}Ca/nHa nanocomposites. *Iran. J. Mater. Sci. Eng.* **2017**, *14*. [[CrossRef](#)]
41. Száraz, Z.; Trojanová, Z.; Cabbibo, M.; Evangelista, E. Strengthening in a WE54 magnesium alloy containing SiC particles. *Mater. Sci. Eng. A* **2007**, *462*, 225–229. [[CrossRef](#)]
42. Choi, S.-M.; Awaji, H. Nanocomposites—A new material design concept. *Sci. Technol. Adv. Mater.* **2005**, *6*, 2. [[CrossRef](#)]
43. Yuan, Q.; Zeng, X.; Wang, Y.; Luo, L.; Ding, Y.; Li, D.; Liu, Y. Microstructure and mechanical properties of Mg-4.0Zn alloy reinforced by NiO-coated CNTs. *J. Mater. Sci. Technol.* **2017**, *33*, 452–460. [[CrossRef](#)]

44. Sanaty-Zadeh, A. Comparison between current models for the strength of particulate-reinforced metal matrix nanocomposites with emphasis on consideration of hall–petch effect. *Mater. Sci. Eng. A* **2012**, *531*, 112–118. [[CrossRef](#)]
45. Sankaranarayanan, S.; Nayak, U.P.; Sabat, R.; Suwas, S.; Almajid, A.; Gupta, M. Nano-zno particle addition to monolithic magnesium for enhanced tensile and compressive response. *J. Alloys Compd.* **2014**, *615*, 211–219. [[CrossRef](#)]
46. Sankaranarayanan, S.; Sabat, R.; Jayalakshmi, S.; Suwas, S.; Gupta, M. Effect of nanoscale boron carbide particle addition on the microstructural evolution and mechanical response of pure magnesium. *Mater. Design* **2014**, *56*, 428–436. [[CrossRef](#)]
47. Parande, G.; Manakari, V.; Meenashisundaram, G.K.; Gupta, M. Enhancing the hardness/compression/damping response of magnesium by reinforcing with biocompatible silica nanoparticulates. *Int. J. Mater. Res.* **2016**, *107*, 1091–1099. [[CrossRef](#)]



© 2018 by the authors. Licensee MDPI, Basel, Switzerland. This article is an open access article distributed under the terms and conditions of the Creative Commons Attribution (CC BY) license (<http://creativecommons.org/licenses/by/4.0/>).